Письма в ЭЧАЯ. 2010. Т. 7, № 3(159). С. 317–330

THE PRIMAKOFF REACTION STUDY FOR PION POLARIZABILITY MEASUREMENT AT COMPASS

A. V. Guskov

Joint Institute for Nuclear Research, Dubna
University of Turin, Department of Physics and Turin Section of INFN, Turin, Italy

The electromagnetic structure of charged pions can be described by the electric (α_π) and magnetic (β_π) polarizabilities that depend on the rigidity of pion's internal structure as a composite particle. It is shown that the values of α_π and β_π can be precisely measured via the Primakoff reaction $\pi^- + (A, Z) \to \pi^- + (A, Z) + \gamma$ in the COMPASS experiment at CERN.

Электромагнитная структура заряженного пиона может быть описана электрической поляризуемостью α_π и магнитной поляризуемостью β_π, которые зависят от жесткости внутренней структуры пиона как составной частицы. Показано, что величины α_π и β_π могут быть точно измерены в реакции примаковского рассеяния $\pi^- + (A, Z) \to \pi^- + (A, Z) + \gamma$ в эксперименте COMPASS в ЦЕРН.

PACS: 13.40.Em; 14.40.Aq; 13.75.Gx

INTRODUCTION

In classical physics the polarizability of a medium or a composite system is the well-known characteristic related to the response of the system to the presence of an external electromagnetic field. If we consider a dipole, the electric polarizability α is the proportionality constant between the electric field and the electric dipole moment, while β is related to the magnetic field and the magnetic dipole moment.

This concept can be extended to the case of composite particles, like pions, kaons and others. In the case of pion, the electric (α_π) and magnetic (β_π) polarizabilities characterize the response of the quark substructure to the presence of an external electromagnetic field in the $\pi\gamma$ Compton-like scattering. These parameters are fundamental ones for any theory describing the pion structure.

The prediction of various theoretical models like chiral perturbation theory, dispersion sum rules, QCD sum rule and quark confinement models for polarizabilities of charged pions are presented in Table 1 (see [1–6]). Different models predict that the $\alpha_\pi + \beta_\pi$ is close to zero while the values for $\alpha_\pi - \beta_\pi$ are in a range $(6{-}14) \cdot 10^{-4}$ fm^3.

Several attempts to measure these quantities were already done using different approaches (see Table 2, [15]). The obtained results are affected by large uncertainties and cannot be used for critic tests of theoretical predictions. New more precise measurements are needed.

Table 1. **Theoretical predictions for** $(\alpha_\pi + \beta_\pi)$ **and** $(\alpha_\pi - \beta_\pi)$

Model	Parameter	10^{-4} fm^3
χPT	$\alpha_\pi - \beta_\pi$ $\alpha_\pi + \beta_\pi$	5.7 ± 1.0 0.16
QCM	$\alpha_\pi - \beta_\pi$ $\alpha_\pi + \beta_\pi$	7.05 0.23
QCD sum rules	$\alpha_\pi - \beta_\pi$	11.2 ± 1.0
Dispersion sum rules	$\alpha_\pi - \beta_\pi$ $\alpha_\pi + \beta_\pi$	13.60 ± 2.15 0.166 ± 0.024

Table 2. **Experimental values of** $\alpha_\pi, \beta_\pi,\ (\alpha_\pi + \beta_\pi),\ (\alpha_\pi - \beta_\pi)$

Data	Reaction	Paramater	10^{-4} fm^3
Serpukhov ($\alpha_\pi + \beta_\pi = 0$) [12] Serpukhov [13]	$\pi Z \to \pi Z \gamma$	α_π $\alpha_\pi + \beta_\pi$ β_π	$6.8 \pm 1.4 \pm 1.2$ $1.4 \pm 3.1 \pm 2.8$ $-7.1 \pm 2.8 \pm 1.8$
Lebedev [7]	$\gamma N \to \gamma N \pi$	α_π	20 ± 12
Mami A2 [14]	$\gamma p \to \gamma \pi^+ n$	$\alpha_\pi - \beta_\pi$	$11.6 \pm 1.5 \pm 3.0 \pm 0.5$
PLUTO [8]	$\gamma\gamma \to \pi^+\pi^-$	α_π	$19.1 \pm 4.8 \pm 5.7$
DM1 [9]	$\gamma\gamma \to \pi^+\pi^-$	α_π	17.2 ± 4.6
DM2 [10]	$\gamma\gamma \to \pi^+\pi^-$	α_π	26.3 ± 7.4
Mark II [11]	$\gamma\gamma \to \pi^+\pi^-$	α_π	2.2 ± 1.6
Global fit: MARK II, VENUS, ALEPH, TPC/2γ, CELLO, BELLE (L. Fil'kov, V. Kashevarov) [15]	$\gamma\gamma \to \pi^+\pi^-$	$\alpha_\pi - \beta_\pi$ $\alpha_\pi + \beta_\pi$	$13.0^{+2.6}_{-1.9}$ $0.18^{+0.11}_{-0.02}$
Global fit: MARK II, Crystal ball (A. Kaloshin, V. Serebryakov) [16]	$\gamma\gamma \to \pi^+\pi^-$	$\alpha_\pi - \beta_\pi$	5.25 ± 0.95

1. PRIMAKOFF REACTION

The Primakoff reaction $\pi^- + (A, Z) \to \pi^- + (A, Z) + \gamma$ can be treated as Compton scattering of the pion off a virtual photon, provided by the nucleus (see Fig. 1). The momentum transferred to the nucleus in the Primakoff reaction is very small ($Q^2 \ll m_\pi^2/c^2$).

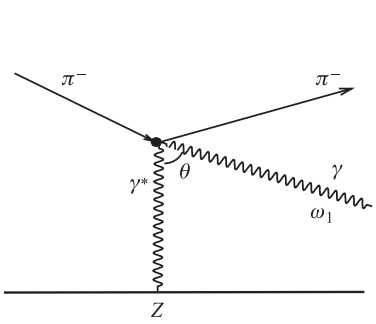

Fig. 1. The diagram of the Compton scattering in inverse kinematics (Primakoff scattering)

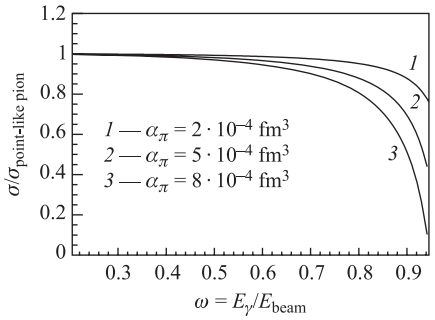

Fig. 2. The Primakoff differential cross section $d\sigma/d\omega$ for different values of pion polarizability α_π

In the anti-laboratory system the differential cross section is described by the formula

$$\frac{d^3\sigma}{dQ\, d\omega_1 d(\cos\,\theta)} = \frac{2\alpha^3 Z^2}{m_\pi^2 \omega_1} \frac{Q^2 - Q^2_{\min}}{Q^4} |F_A(Q^2)|^2 \times \\ \times \left(F^{\text{Pt}}_{\pi\gamma} + \frac{m_\pi \omega_1^2}{\alpha} \frac{\alpha_\pi(1+\cos^2\theta) + 2\beta_\pi \cos\,\theta}{(1+(\omega_1/m_\pi)(1-\cos\,\theta))^3} \right), \quad (1)$$

where $Q^2_{\min} = (m_\pi \omega_1 / p_{\text{beam}})^2$, m_π is the pion mass; ω_1 is the energy of the virtual photon; θ is the angle between the real photon and the virtual photon directions; $F_A(Q^2)$ is the electromagnetic form factor of the nucleus ($F_A(Q^2) \approx 1$ for $Q \ll m_\pi/c$); α is the fine structure constant; $F^{\text{Pt}}_{\pi\gamma}$ [17] is the differential Compton cross section for the scattering of photons on a point-like spin-0 particle. The cross section depends on $\alpha_\pi + \beta_\pi$ at forward angles and on $\alpha_\pi - \beta_\pi$ at backward angles. So, via measurements of the cross section (Eq. (1)) vs. the photon energy and the scattering angle, one can extract both α_π and β_π.

All the theoretical models mentioned above predict that

$$\alpha_\pi + \beta_\pi \ll \alpha_\pi - \beta_\pi \quad (2)$$

and performed experiments (see Table 2) confirm it. So, to begin with, one can perform the measurement of the pion polarizabilities under assumption that

$$\alpha_\pi + \beta_\pi = 0. \quad (3)$$

In this case to extract pion polarizability α_π it is enough to compare the measured differential cross section $d\sigma/d\omega_1$ or $d\sigma/d(\cos\,\theta)$ and theoretically predicted for the point-like (unstructured) pion. Due to the small scattering angles in the laboratory system (typical angles are $\sim m_\pi/E_0$, where E_0 is the energy of incoming pion), the relative precision of angular measurements is much lower than the relative precision of photon energy measurement. Therefore, the study of energy spectrum of scattered photons is preferable and the laboratory system is more convenient for such kind of studies.

Using the ω variable, which is the relative energy of emitted photon in lab. system:

$$\omega = E_\gamma / E_0, \quad (4)$$

the ratio R of the differential cross section $d\sigma/d\omega$ for pion with polarizability α_π to the corresponding differential cross section for the point-like pion (Born cross section) can be approximately expressed as [20]

$$R = 1 - \frac{3}{2}\frac{\omega^2}{1-\omega}\frac{m_\pi^3}{\alpha}\alpha_\pi. \tag{5}$$

The ratios R for the different values of α_π are presented in Fig. 2, from which one can see that the most visible effects of the polarization correspond to large values of ω.

2. THE GENERAL REQUIREMENTS ON THE EXPERIMENTAL SETUP FOR PRIMAKOFF REACTION STUDIES

Peculiarities of the Primakoff reaction put the general requirements for the experimental setup, strategy of data taking and analysis.

2.1. Target. In addition to the scattering of pions in the electromagnetic field of nucleus, there is a nuclear diffractive scattering with the same signature but for which the momentum transfer is much larger. The diffractive scattering produces a significant contribution to a counting rate in the region of large Q^2, while the Primakoff events are peaked at $Q^2 \simeq 0$. To separate Primakoff and diffractive scattering, the experimental setup must have a good resolution in Q^2. Multiple scattering in a target material is one of the main sources of uncertainties in Q^2 measurement and it limits the thickness of the target. One should also take into account the probability of Primakoff photon lost due to its conversion into e^+e^- pair within the target, which decreases the acceptance. So, the thickness of the target should be much less than one radiation length.

To optimize the ratio of Primakoff signal, which is proportional to Z^2, to diffractive background, the material with large Z is preferable for the target. But Z should not be too large to minimize radiative corrections to the Born cross section [21–24]. These corrections and corresponding systematic shifts of α_π are shown in Figs. 3 and 4. Corrections for Compton vertex, multiple photon exchange, vacuum polarization, electromarnetic form factor of nucleus and nuclear charge screening by electrons are taken into account.

2.2. Beam. The cross section of Primakoff scattering weakly depends on the energy of incoming pion. For the point-like pion it can be expressed as

$$\frac{d\sigma}{d\omega} = \frac{4Z^2\alpha^3}{m_\pi^2}\frac{1-\omega}{\omega}\left(\frac{2}{3}\ln\frac{Q^2_{\max}}{Q^2_{\min}} - \frac{19}{9} + 4\sqrt{\frac{Q^2_{\min}}{Q^2_{\max}}}\right), \tag{6}$$

where

$$Q_{\min} = \frac{\omega m_\pi^2}{2E_{\mathrm{beam}}(1-\omega)} \tag{7}$$

and $Q_{\max}$ can be chosen taking into account the setup resolution for Q^2. So, variation of the beam energy does not change significantly the cross section and therefore the statistics. But the scale of energies of incoming and outgoing particles determines the quality of collected data. For instance, for small energies the multiple scattering in the target material creates a significant problem, while for high energies small scattering angles of the photon make worse the resolution in Q^2. So the beam energy should be optimized in each particular case with

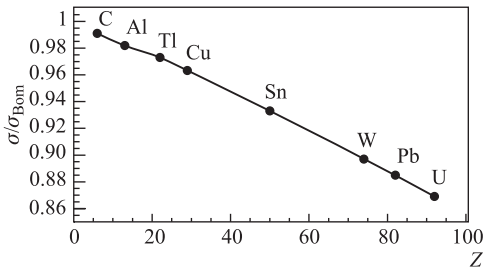

Fig. 3. Radiative corrections to the Primakoff cross section as a function of Z

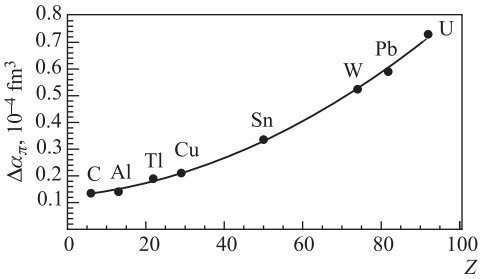

Fig. 4. Systematic shifts of α_π due to radiative corrections for different Z

respect to such parameters of a setup as the spatial resolution of tracking detectors, the spatial and energetic resolution of the electromagnetic calorimeter, the amount of the material in the beam line (including target), etc.

As for the sign of the beam pions, the positive and negative pions are equivalent. But in practice it is simpler to form the beam of negative pions, where the admixture of other particles is small enough. Positive beams are usually contaminated by protons.

2.3. Detector. The configuration of Primakoff events requires the precise tracking up- and downstream of the target to measure the pion scattering angle, an electromagnetic calorimeter to measure energy and position of the photon cluster and a magnetic spectrometer for scattered pion momentum measurement. Taking into account that it is difficult to form pure pion beam, the setup should have possibilities to identify incoming and outgoing particles.

2.4. Trigger. A hard photon in the final state is the most important signature of Primakoff reaction. So, the significant energy deposition in the electromagnetic calorimeter can be the main requirement for the Primakoff trigger.

3. PION POLARIZABILITIES MEASUREMENT IN SERPUKHOV

The first measurement of pion polarizabilities via the Primakoff reaction was proposed in [18] and performed with the SIGMA–AYAKS spectrometer (Fig. 5) in Serpukhov in the 40 GeV/c negative beam [12, 13, 19, 20]. Beam particles were identified by the differential and threshold gas Cherenkov counters and their tracks were measured by hodoscopes and proportional chambers. The main statistics was collected with $0.25X_0$ carbon target (T), but Be, Al, Fe, Cu and Pb targets were also used. The scattered pions were detected by the magnetic spectrometer. The gas Cherenkov counter C_2 was used to set the upper limit on scattered π^- momenta ($P_{\max} = 18$ GeV/c). The energy and the position of the photons were measured by 80 lead glass Cherenkov counters (C_{80}). Guard counters (R, G, F) were used to identify the events with large scattering angle. A system of 50 lead glass Cherenkov counters C_{50} was used to suppress possible beam electron bremsstrahlung. The trigger required the energy deposition in the lead glass counters above 5 GeV, no signals from guard counters, and a signal produced by scattered pion in the hodoscope.

The following criteria were used for offline selection of Primakoff events:

- only one negative particle with the momentum 4–18 GeV/c detected in the spectrometer;
- the pion scattering angle greater than 1.5 mrad;

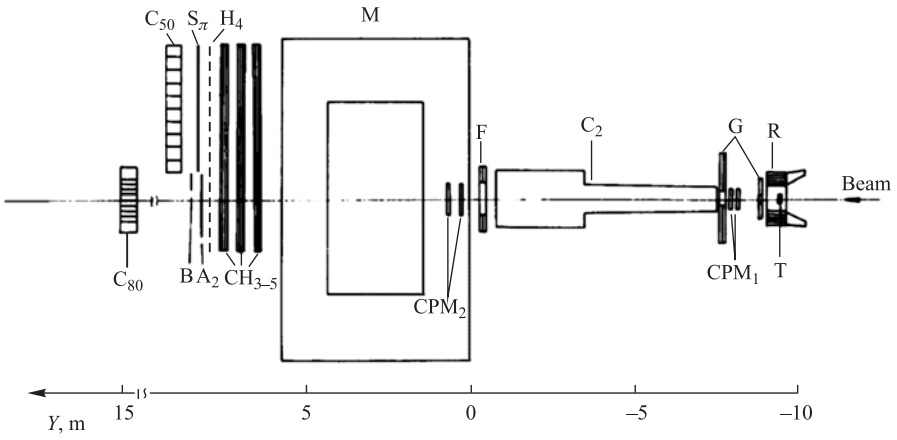

Fig. 5. Layout of the SIGMA–AYAKS spectrometer

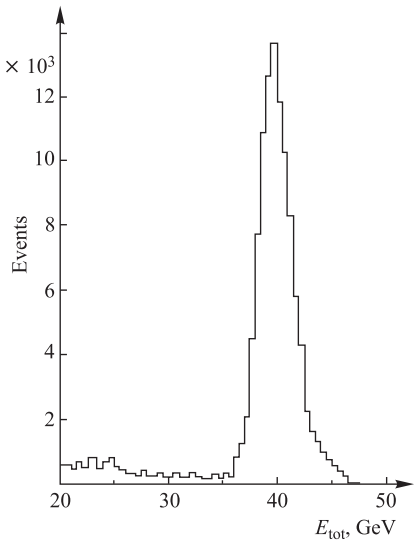

Fig. 6. The distribution for $E_{\rm tot} = E_\gamma + E_\pi$ in the experiment SIGMA–AYAKS [12]

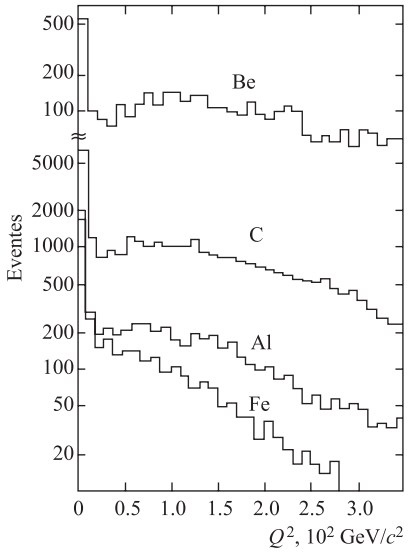

Fig. 7. The Q^2-distributions for different targets in the experiment SIGMA–AYAKS [12]

- the tracks of incident and scattered pions crossing in the target;
- only one photon detected in C_{80};
- $35 < E_\gamma + E_\pi < 45$ GeV (exclusivity requirement);
- $Q^2 < 6 \cdot 10^{-4}$ (GeV/c)^2.

The main parameters of the spectrometer are presented in Table 3. Figures 6 and 7 show the exclusivity peak and Q^2-distributions for different target materials. The total Primakoff statistics collected with all targets was about 6000 events that allowed one to measure pion

Table 3. **Comparison of SIGMA–AYAKS and COMPASS spectrometers**

Parameters	SIGMA–AYAKS	COMPASS 2004
Beam particles	π^-	π^-, μ^-
Beam momentum, GeV/c	40	190
Composition of the hadrom beam, %:		
π^-	95	93.5
K^-	2.1	3
μ^-	2.5	3
p^-	0.3	0.5
e^-	0.1	~ 0.1
Beam intensity, s^{-1}	10^6	$10^6(\pi),\ 4 \cdot 10^6(\mu)$
Beam momentum spread, %	2.5	0.7(π), 4(μ)
Main target, X/X_0	0.25(C)	0.5(Pb)
Other targets	Be, Al, Fe, Cu, Pb	C, Cu
Resolution for the vertex position, mm:		
X, Y	—	0.5
Z	—	$5 + 30/\theta_\pi$
Resolution for scatt. pion momentum, %	1	0.3–0.4
Resolution for angle of incoming and scattering pion, mrad	0.12	0.01
Resolution for photon angle, mrad	0.12	0.06
Resolution for photon energy, %	3.5 for 26.6 GeV	5 for $>$ 100 GeV
Resolution for Q, MeV/c	12	18
Resolution for $E_{\rm tot}$, %	5	3
Double photon resolution, mrad	—	1.5
Primakoff trigger rates, kHz	~ 0.01	10 (Primakoff 1) 7 (Primakoff 2)
Total beam flux	$1.2 \cdot 10^{11}$	$10^{11}(\pi),\ 7 \cdot 10^{10}(\mu)$
Collected statistics ($0.5 < \omega < 0.9$)	$6 \cdot 10^3$	$3 \cdot 10^4$

polarizability α_π under assumption $\alpha_\pi + \beta_\pi = 0$ with the statistical error $1.4 \cdot 10^{-4}$ fm^3 and systematic error $1.2 \cdot 10^{-4}$ fm^3. Independent estimation of α_π and β_π was performed with the statistical accuracy $2.8 \cdot 10^{-4}$ fm^3 and systematic accuracy $1.8 \cdot 10^{-4}$ fm^3. The contribution to the result from the radiative correction was estimated to be about $0.2 \cdot 10^{-4}$ fm^3 [23].

4. PRIMAKOFF REACTION STUDIES AT COMPASS

COMPASS is the experiment in the secondary beam line M2 of Super Proton Synchrotron (SPS) at CERN, along which the high energy beams of muons and hadrons are formed and directed to the experimental hall. The purpose of this experiment is the study of hadron structure and hadron spectroscopy with high intensity muon and hadron beams [25]. The COMPASS setup (Fig. 8, Table 3) provides unique conditions for investigation of the Primakoff processes [26–29]. It has silicon detectors up- and downstream of the target with

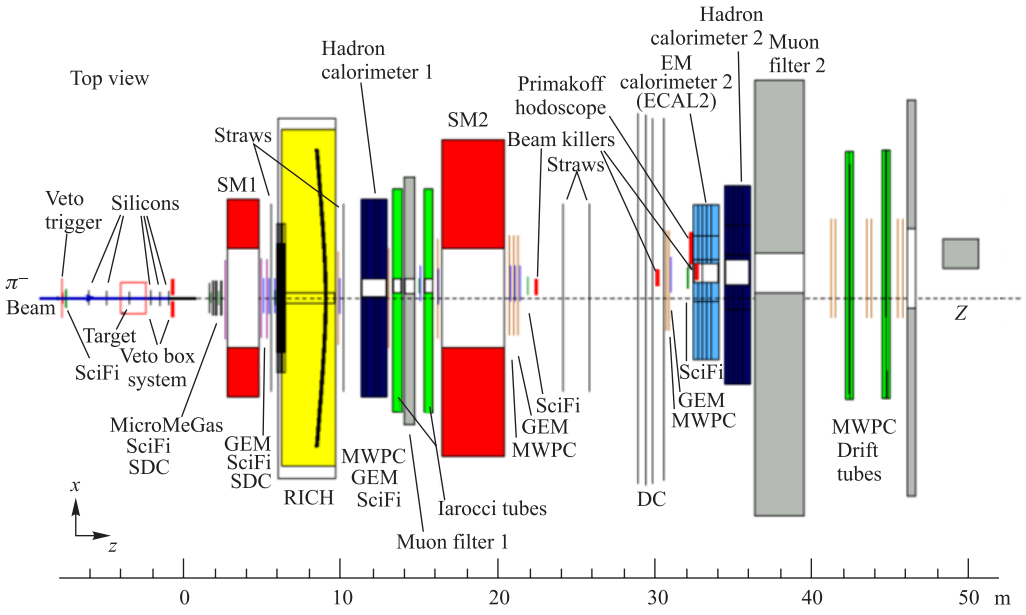

Fig. 8. Layout of the COMPASS setup 2004

a spatial resolution of about 10 μm for the precise vertex position reconstruction and for the measurement of the pion scattering angle, an electromagnetic calorimeter for the photon 4-momentum reconstruction (spatial resolution for $E > 100$ GeV is about 1.5 mm, energy resolution is $\sim 5\%$ for $E > 100$ GeV) and two magnetic spectrometers for the determination of the scattered pion momentum ($dP/P < 0.5\%$). Hadron calorimeters and muon identification system are used for identification of secondary particles.

In COMPASS there is a unique possibility to study the reaction with a μ^- beam:

$$\mu^- + (A, Z) \to \mu^- + (A, Z) + \gamma. \tag{8}$$

Since the muon is a point-like particle, the ratio of the measured differential cross section to the calculated cross section (taking into account that spin of muon is $1/2$) has to be equal to unity within the errors for all values of ω. This is the best way to estimate systematic uncertainties.

Taking into account the experience of Serpukhov experiment, using the power of the modern technologies, methods of high energy physics and computing facilities, one can perform the measurement of pion polarizabilities with higher precision, compared to previous experiments.

The comparison of the SIGMA–AYAKS and COMPASS spectrometers for the Primakoff reaction studies is given in Table 3.

4.1. Primakoff Reaction Study During the Pilot Hadron Run 2004. The possibilities of the Primakoff reaction studies at COMPASS were estimated using the data collected with the 190 GeV/c π^- beam and Pb target of 3 mm, $2 + 1$ mm ($0.5X_0$) and 1.6 mm ($0.3X_0$) thickness during the pilot hadron run [30–32]. Additional samples with Cu ($0.25X_0$), C ($0.12X_0$) and

empty targets were used to study background processes and systematic errors. Sample with a 190 GeV/c μ^- beam and $2+1$ mm Pb target was also collected.

Two types of trigger were used for the selection of Primakoff events: Primakoff 1 and Primakoff 2. Trigger Primakoff 1 required a beam particle, a hit in the Primakoff hodoscope, produced by scattered pion, energy deposition in the electromagnetic calorimeter (ECAL2) above 45 GeV, no energy deposition in the first hadron calorimeter above 6 GeV, no energy deposition in the second hadron calorimeter above 18 GeV and no signals in veto detectors (beam killers, veto system). As was found later, this trigger was too complex to be precisely described in the Monte Carlo simulation and was not used in the final analysis. Trigger Primakoff 2 required the energy deposition in the ECAL2 above 90 GeV and no signal in veto detectors.

Monte Carlo simulation of the setup was based on the POLARIS generator [33] for production of Primakoff events and GEANT 3.21 for the detector simulation.

It was found from the analysis that for selection of candidates to Primakoff events, the following criteria are the most effective:

- only one negative particle reconstructed in the spectrometer, which produced at least 10 hits in 12 planes of silicon detectors;
- reconstructed vertex is close to the nominal position of the target;
- only one cluster in the ECAL2 with $E > 7$ GeV, which is not associated with the track of charged particle. This requirement removes clusters from pile-up of events and electronic noise;
- $|E_{\rm beam} - E_\gamma - E_\pi| < 25$ GeV;
- $Q^2 < 2 \cdot 10^{-3}$ (GeV/c)^2.

To obtain pure sample of Primakoff events, additional cuts were used to exclude the background events with the same signature.

4.2. Study of the Background Processes. There are few background reactions which have the same signature in COMPASS detector as the Primakoff reaction:

$$A^- \to B^- + \text{ECAL2 cluster}\,(E > 7\ \text{GeV}),$$

where A^- is the beam particle; B^- is the scattered negatively charged particle and ECAL2 cluster is due to neutral particle.

Background processes can be classified into five groups:

1. Diffractive $\pi^- + \text{Pb} \to \text{Pb} + \pi^- + \gamma$ events. They typically have large Q^2 and can be effectively rejected by the Q^2 cut. This background in visible from the comparison of Q^2-distributions of events, produced by pions and muons (Fig. 9). To take into account the background from diffractive scattering under the Primakoff peak, one can fit it with an exponential function in the range of large Q^2 and extrapolate the fitted curve to $Q^2 = 0$. One should also pay attention to the interference of the Primakoff and diffractive amplitudes.

2. Events with beam particles different from pion:

$$\mu^- + \text{Pb} \to \mu^- + \text{Pb} + \gamma,$$
$$e^- + \text{Pb} \to e^- + \text{Pb} + \gamma,$$
$$p^- + \text{Pb} \to p^- + \text{Pb} + \gamma,$$
$$K^- + \text{Pb} \to K^- + \text{Pb} + \gamma.$$

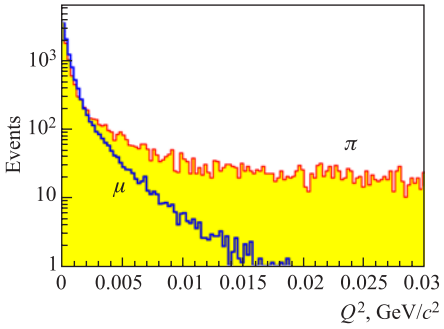

Fig. 9. The Q^2-distributions of events, produced in pion and muon beams

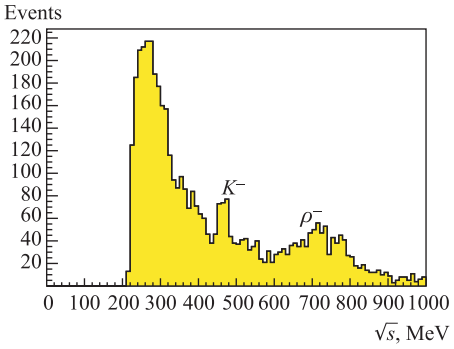

Fig. 10. The $\pi\gamma$-invariant mass. Background from K^- and ρ^- decay is visible

Because of the relatively big mass and small admixture in the hadron beam, the kaon and proton backgrounds are negligible. Beam muons and electrons are the most important sources of background.

Background from muons can be reduced by rejection of the events with scattered particles identified as muons by the muon identification system.

As for electron background, typical Primakoff scattering angle for electron is about $m_e/E_{\rm beam} \approx 0.003$ mrad which is much smaller than the angle of multiple scattering in the target material (0.07 mrad). Cut on the P_t of outgoing charged particle is very effective against $e\gamma$ events. In the present analysis the events with $P_t < 45$ MeV/c were rejected.

3. Events with π^0, one soft decay photon of which was lost or two photons produced one cluster in ECAL2:

$$\begin{aligned}
&\pi^- + \mathrm{Pb} \to \pi^- + \mathrm{Pb} + \pi^0 \to \pi^- + \mathrm{Pb} + \gamma + \gamma \ (\mathrm{Primakoff}),\\
&\pi^- + \mathrm{Pb} \to \pi^- + \mathrm{Pb} + \pi^0 \to \pi^- + \mathrm{Pb} + \gamma + \gamma \ (\mathrm{diffractive}),\\
&\pi^- + \mathrm{Pb} \to \rho^- + \mathrm{Pb} \to \mathrm{Pb} + \pi^- + \pi^0 \to \pi^- + \mathrm{Pb} + \gamma + \gamma,\\
&\qquad K^- \to \pi^- + \pi^0 \to \pi^- + \gamma + \gamma,\\
&K^- + \mathrm{Pb} \to K^*(892) + \mathrm{Pb} \to \mathrm{Pb} + K^- + \pi^0 \to \mathrm{Pb} + K^- + \gamma + \gamma.
\end{aligned}$$

These events can be rejected using the calorimeter information. Particularly, analyzing the cluster shape, one can reject the events with two photons in one cluster. One can also recover the clusters of the lost soft photons analyzing the noise and pile-up clusters. For this purpose the events are rejected if they have additional clusters with $E > 1.5$ GeV and the invariant mass of two photons, associated with calorimeter clusters, is close to π^0 mass. Since the decay of beam kaons take place anywhere along the beam line, for studies of this background one can choose the events with vertices placed outside (up- and downstream) of the target. It will be the pure sample of $\pi^-\pi^0$ events, mis-identified as $\pi^-\gamma$ events. This sample is used to control the efficiency of π^0 background suppression. Background from kaon and ρ-meson decay is visible in Fig. 10.

The cut on $\pi^-\gamma$-invariant mass is also effective against the π^0 from ρ-meson decay. For the COMPASS setup the events with $M_{\pi\gamma} > 3.75\ m_\pi$ should be rejected.

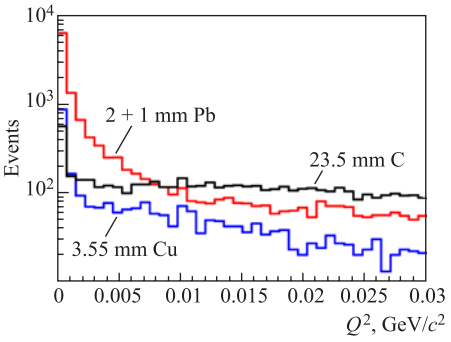

Fig. 11. The Q^2-distributions for led, copper and carbon targets

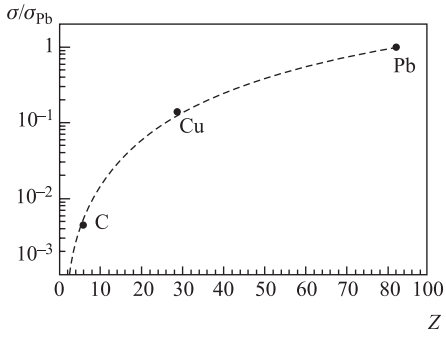

Fig. 12. The Z^2-dependence of Primakoff cross section

4. Double bremsstrahlung events $\pi^- \to \pi^- + \gamma + \gamma$ with double photon clusters or with one lost soft photon. Their contribution is taken into account in the radiative correction for Compton vertex.

5. Events with hard photon and soft lost π^0 in the final state:

$$\pi^- + \mathrm{Pb} \to \rho^- + \gamma + \mathrm{Pb} \to \mathrm{Pb} + \pi^- + \pi^0 + \gamma.$$

The cross section of such a process is two orders of magnitude less than the cross section of ρ-meson production without photon emission, but this background cannot be rejected by the cut on $M_{\pi\gamma}$. The low threshold of photon registration in ECAL2 can help to reject such events.

4.3. Primakoff Scattering on Different Nuclear Targets. The comparison of data samples collected with different targets provides the possibility to see the Q^2 behavior of the Primakoff signal and diffractive scattering background for different materials and to check the Z^2-dependence for the Primakoff cross section. In Fig. 11 one can see that Primakoff signal at $Q^2 = 0$ increases with increasing Z. The shape of the Primakoff peak can be described by exponential function

$$N(Q^2) = N(0) \exp\left[-\frac{Q^2}{(dQ)^2}\right], \tag{9}$$

where dQ is the resolution of the setup for the transferred momentum (see Table 3). The Primakoff cross sections for different materials normalized to the cross section for lead is shown in Fig. 12. The dotted line corresponds to Z^2-dependence. One can see that the measured values satisfy the Z^2-dependence rule for a wide range of Z. This proves that selection criteria effectively select Primakoff events and reject background events.

4.4. Estimation of Possible Statistical and Systematic Uncertainties of Pion Polarizabilities Measurement at COMPASS under Assumption $\alpha_\pi + \beta_\pi = 0$. The statistics of the Primakoff events, collected during the test hadron run in the range $0.5 < \omega < 0.9$ is about 30 000 events (total flux is 10^{11} pions). Corresponding statistical error of α_π measurement is $0.9 \cdot 10^{-4}$ fm^3. But the bigger part of the statistics was collected under unstable conditions of the detector operation that introduce additional systematic uncertainties. The estimated contributions to the systematic error from the different background processes are presented in Table 4.

Table 4. **The estimations of the systematic uncertainties for the $2+1$ mm Pb target**

Estimation of systematic errors	Error, 10^{-4} fm^3
Subtraction of diffractive background	± 0.2
Subtraction of π^0 background	± 0.3
Background from $\mu^- + A \to \mu^- + A + \gamma$	$+0.2$
Background from $e^- + A \to e^- + A + \gamma$	$< +0.1$
Setup performance and MC	> 0.5
Total systematic error	> 0.65

It is important to emphasize that the systematic uncertainties related to subtraction of the diffractive background and the background of the events with π^0 have the statistical nature and decrease with increasing of the statistics. That is true also for the lower limit of the contribution to systematics of the setup performance and the quality of the Monte Carlo description, which can be tested using data collected with the muon beam.

4.5. Possibility of Future Measurements at COMPASS. The pilot hadron run 2004 has shown that the COMPASS setup provides good opportunity to measure pion polarizabilities with the precision inaccessible for previous experiments. To increase statistics and improve the quality of collected data, some modifications of the setup should take place with respect to 2004:

• beam intensities should be increased to $2 \cdot 10^7$ pions per 10 s spill of SPS and $2 \cdot 10^8$ muons per spill compatible with the trigger and DAQ capabilities;

• optimized electron converter should be installed in the beam line to reduce the admixture of electrons in the pion beam;

• threshold Cherenkov detector (CEDAR) should be used for the beam kaons identification;

• $0.5X_0$ Pb target should be replaced by $0.3X_0$ Ni target to reduce the influence of the corrections to the Born cross section and improve resolution for Q^2;

• Primakoff 2 trigger should be used and include only the central part of the electromagnetic calorimeter with the threshold about 30–40 GeV to enrich the collected statistics by Primakoff events;

• identification of scattered charged particle should be improved.

With such modifications the data collected during one month of new data taking will correspond to the total flux of $8 \cdot 10^{11}$ for pion and muon beams. The number of Primakoff events will be about 200 000 in the range $0.5 < \omega < 0.9$. It corresponds to the statistical error of α_π measurement under assumption $\alpha_\pi + \beta_\pi = 0$ to be about $0.33 \cdot 10^{-4}$ fm^3. The lowest possible systematic uncertainty, based on the data to be collected with muon beam, is $0.16 \cdot 10^{-4}$ fm^3. With such a precision for the first time one can critically test the theoretical predictions.

The large statistics will provide also possibilities for:

• the independent measurement of α_π and β_π with a statistical error of about $0.5 \cdot 10^{-4}$ fm^3;

• the measurement of the pion polarizability not only averaged in $M_{\pi\gamma}$-range below some limit, as it was done before, but also for the measurement of the dynamic polarizability $\alpha_\pi(M_{\pi\gamma})$ in the range of $M_{\pi\gamma}$ up to ~ 0.55 GeV [34];

• the tests of the α_π dependence on ω, predicted by some theoretical models.

In addition to precise measurement of pion palarizabilities, COMPASS have a chance to be the first in observation of Primakoff scattering of charged kaons [27, 35]. As far as the Primakoff cross section for kaons is $m_K^2/m_\pi^2 \approx 12.5$ times smaller than for pions and the fraction of kaons in the beam is about 3%, the statistics, collected with kaons, can rich about 500 events per month. It is enough for the first estimation of the kaon polarizabilities.
Other Primakoff reactions like $\pi^- + (A, Z) \to \pi^- + \pi^0 + (A, Z)$, hybrid mesons production, etc. (see [28] and [36]) can also be studied.

Acknowledgements. I wish to thank the COMPASS collaboration, Munich and Turin groups, deeply involved into the Primakoff analysis, especially M.-L. Colantoni, O. Denisov, A.-M. Dinkelbach, J. Friedrich, T. Nagel and D. Panzieri for the contribution into this work and comprehensive discussion of the results. I am also grateful to Z. Krumshtein, A. Nagaitsev, A. Olshevski and I. Savin for the support of this work.

REFERENCES

1. *Portoles J., Pennington M. R.* The Second DaΦne Physics Handbook. V. 2. 1999. P. 579.
2. *Wilmot C. A., Lemmer R. H.* // Phys. Rev. C. 1994. V. 65. P. 035206.
3. *Pervushin V. N., Volkov M. K.* // Phys. Lett. B. 1975. V. 55. P. 406.
4. *Radzhabov A. E., Volkov M. K.* // Part. Nucl., Lett. 2005. V.2, No. 1(124). P. 7–12.
5. *Gasser J., Ivanov M. A., Sainio M. E.* // Nucl. Phys. B. 2006. V.745. P. 84.
6. *Walcher T.* // Physik J. 2006. V. 5. P. 45.
7. *Aibergenov T. A. et al.* // Czech. J. Phys. B. 1986. V. 36. P. 948.
8. *Berger C. et al.* // Z. Phys. C. 1984. V. 26. P. 199.
9. *Courau A. et al.* // Nucl. Phys. B. 1986. V. 271. P. 1.
10. *Ajaltoni Z. et al.* // VII Intern. Workshop on Photon–Photon Collision. Paris, 1986.
11. *Boyer J. et al.* // Phys. Rev. D. 1990. V. 42. P. 1350;
Babusci D. et al. // Phys. Lett. B. 1992. V. 277. P. 158.
12. *Antipov Yu. M. et al.* // Phys. Lett. B. 1983. V. 121. P. 445.
13. *Antipov Yu. M. et al.* // Z. Phys. C. 1985. V. 26. P. 495.
14. *Ahrens J. et al.* // Eur. Phys. J. A. 2005. V. 23. P. 113.
15. *Fil'kov L. V., Kashevarov V. L.* // Phys. Rev. C. 2006. V. 73. P. 035210.
16. *Kaloshin A. E., Serebryakov V. V.* // Z. Phys. C. 1994. V. 64. P. 689.
17. *Buenerd M.* // Nucl. Phys. A. 1995. V. 361. P. 111.
18. *Galperin A. S. et al.* // Yad. Fiz. 1980. V. 32. P. 1053.
19. *Antipov Yu. M. et al.* // Phys. Lett. B. 1983. V. 121. P. 445.
20. *Antipov Yu. M. et al.* JINR Preprint P1-86-710. Dubna, 1986.
21. *Arbuzov A. B.* // JHEP. 2008. V. 01. P. 031.
22. *Akhundov A. A. et al.* // Z. Phys. C. 1995. V. 66.
23. *Akhundov A. A. et al.* JINR Preprint P1-86-710. Dubna, 1986.
24. *Kaiser N., Friedrich J. M.* // Eur. Phys. J. A. 2009. V. 39. P. 71.
25. *Bradamante F. et al.* CERN Proposal COMPASS. CERN/SPSLC 96-14, SPSC/P297, CERN/SPSLC 96-30, SPSC/P297. Addendum 1.

26. *Abbon P. et al.* // Nucl. Instr. Meth. A. 2007. V. 577. P. 455.
27. *Moinester M. A. et al.* // Czech. J. Phys. B. 2003. V. 53. P. 169.
28. *Moinester M. A.* Pion Polarizabilities and Hybrid Meson Structure at COMPASS. Tel Aviv University Preprint TAUP 2661-2000; hep-ex/0012063.
29. *Olchevski A., Faessler M.* Experimental Requirements for COMPASS Initial Primakoff Physics Program // COMPASS Collab. Meeting, 2001.
30. *Guskov A. (COMPASS Collab.)* // Fizika B. 2008. V. 17. P. 313.
31. *Guskov A.* // J. Phys. Conf. Ser. 2008. V. 10. P. 022016.
32. *Guskov A. (COMPASS Collab.)* // ICHEP 2006, Moscow, 2006. P. 655.
33. *Buenérd M.* // Nucl. Instr. Meth. A. 1995. V. 361. P. 111.
34. *Kaiser N., Friedrich J.* // Eur. Phys. J. A. 2008. V. 36. P. 181.
35. *Guerrero F., Prades J.* // Phys. Lett. B. 1997. V. 405. P. 341.
36. *Moinester M. A., Steiner V.* hep-ex/9801011.

Received on September 8, 2009.